From: Dominika Phillips
To: Hornsea Project Three; KJ Johansson; Kay Sully
Cc: Andrew Guyton; Stuart Livesey
Subject: Hornsea Project Three (UK) Ltd response to Deadline 4 (Part 12)
Date: 15 January 2019 23:18:39
Attachments: image001.png
D4_HOW03_Appendix 49_Roulund et al 2019a.pdf
D4_HOW03_Appendix 50_Roulund et al 2019b.pdf
D4_HOW03_Appendix 51_Defra MCZ Guidance 2010.pdf
D4_HOW03_Appendix 53_WQ_2.1.3.pdf
D4_HOW03_Appendix 54_ Aviation Assessments.pdf
D4_HOW03_Appendix 55_Development Principles_rev2.pdf
D4_HOW03_Appendix 56_Manwell et al 2009.pdf
D4_HOW03_Appendix 57_Helideck Certificates.pdf
D4_HOW03_Appendix 58_Indicative Array Layout.pdf
D4_HOW03_Appendix 59_FCLP_rev3.pdf
D4_HOW03_Appendix 60_Draft CfD Budget Notice.pdf
D4_HOW03_Appendix 62_Q2.2.34.pdf
D4_HOW03_Appendix 63_Q2.2.7_Q2.2.44.pdf
D4_HOW03_Appendix 64_Dogger Bank.pdf

Dear Kay, K-J

Please find attached the 12th instalment of documents.

Best regards,
Dr Dominika Chalder PIEMA
Environment and Consent Manager

[redacted]

Environmental Management UK| Wind Power
5 Howick Place | London | SW1P 1WG

Ørsted

Hornsea Project Three
Offshore Wind Farm

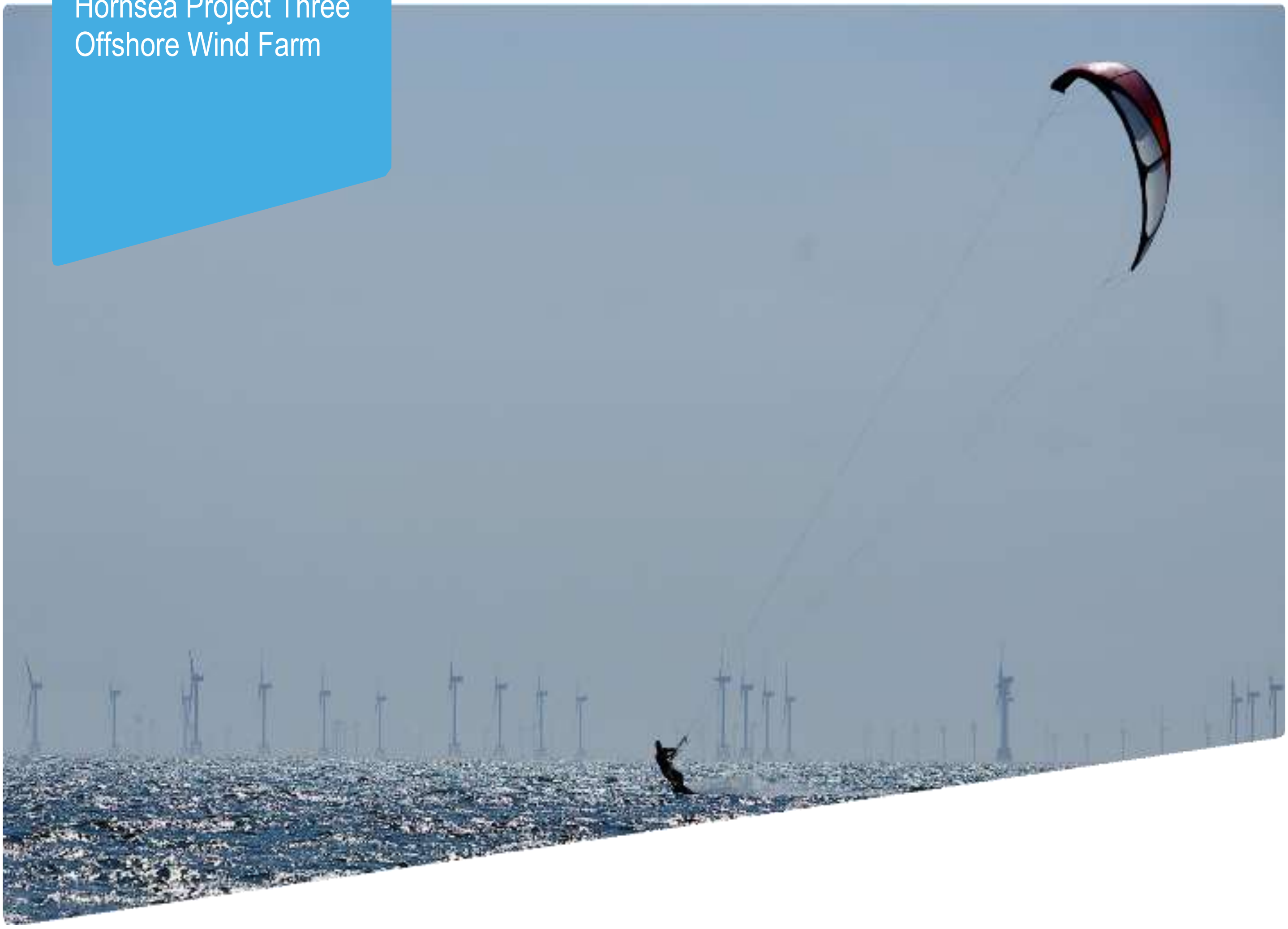

Hornsea Project Three

Offshore Wind Farm

Appendix 56 to Deadline 4 Submission – Manwell et al., 2009

Date: 15th January 2019

Hornsea 3
Offshore Wind Farm

Ørsted

Document Control			
Document Properties			
Organisation	Ørsted Hornsea Project Three		
Author	Manwell et al., 2009		
Checked by	n/a		
Approved by	n/a		
Title	Appendix 56 to Deadline 4 Submission – Manwell et al., 2009		
PINS Document Number	n/a		
Version History			
Date	Version	Status	Description / Changes
15/01/2019	A	Final	Submitted at Deadline 4 (15/01/2019)

Ørsted

5 Howick Place,

London, SW1P 1WG

J.F. MANWELL | J.G. MCGOWAN | A.L. ROGERS

WIND ENERGY EXPLAINED

THEORY, DESIGN AND APPLICATION

SECOND EDITION

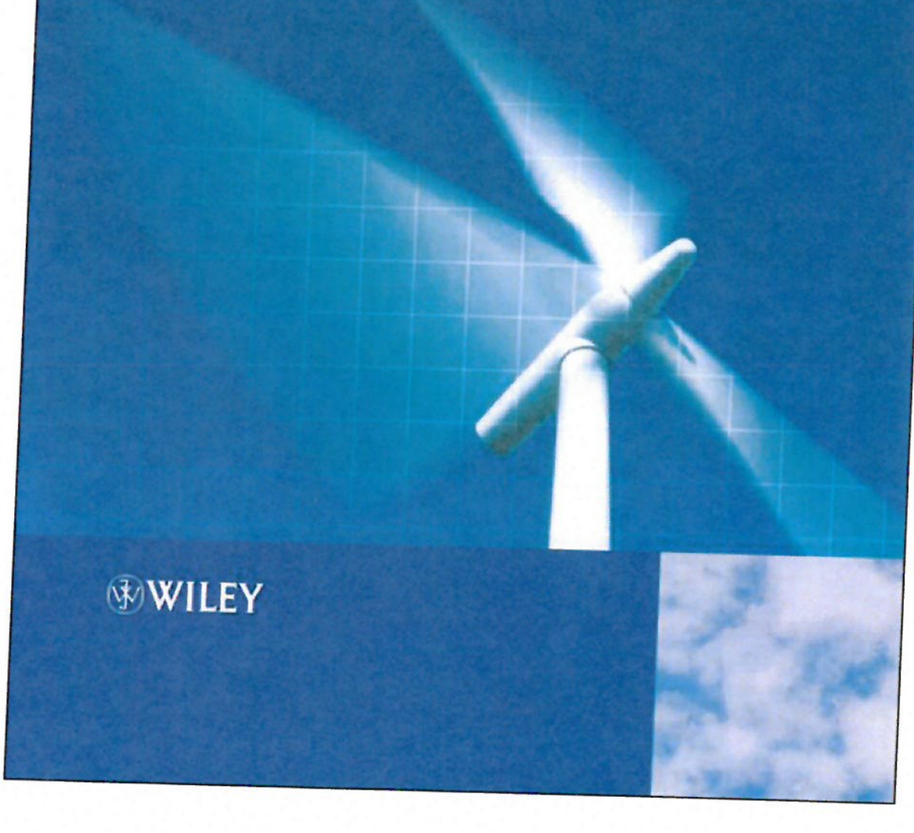

WILEY

turbines, or one individual turbine can be displayed. The information typically includes turbine operating states, power level, total energy production, wind speed and direction, and maintenance and repair notes. SCADA systems also display power curves or graphs of other information and allow system operators to shut down and reset turbines. Newer SCADA systems connected to modern turbines may also display oil temperatures, rotor speed, pitch angle, etc. SCADA systems also provide reports on turbine and wind farm operation to system operators, including information on operation and revenue from each turbine based on turbine energy production and utility rate schedules.

9.4.1.4 Support Personnel

Once a certain number of turbines are placed in a wind farm, it becomes economical to provide dedicated operating and maintenance staff, sometimes called 'windsmiths.' The staff needs to be appropriately trained and provided with suitable facilities.

9.4.2 Wind Farm Technical Issues

Numerous technical issues arise with the close spacing of multiple wind turbines. The most important are related to the question of where to locate and how closely to space the wind turbines (common terms for referring to wind turbine array spacing are illustrated in Figure 9.5). As mentioned in Section 9.2, the wind resource may vary across a wind farm as a result of terrain effects. In addition, the extraction of energy by those wind turbines that are upwind of other turbines results in lower wind speeds at the downwind turbines and increased turbulence. As described in this section, these wake effects can decrease energy production and increase wake-induced fatigue in turbines downwind of other machines. Wind turbine spacing also affects fluctuations in the output power of a wind farm. As described in Section 9.5, the fluctuating power from a wind farm may affect the local electrical grid to which it is attached. This section describes the relationship between wind farm output power fluctuations and the spacing of the turbines in a wind farm.

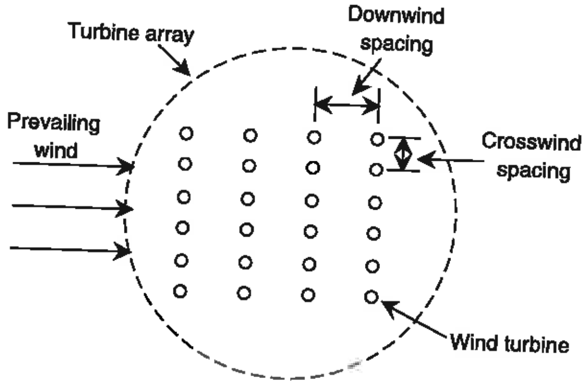

Figure 9.5 Wind farm array schematic

9.4.2.1 Array Losses

Wind energy comes from the conversion of kinetic energy in the wind. This results in lower wind speeds behind a wind turbine and less energy capture by the downstream turbines in an array. Thus, a wind farm will not produce 100% of the energy that a similar number of isolated turbines would produce in the same prevailing wind. The energy loss is termed 'array loss.' Array losses are mainly functions of:

- wind turbine spacing (both downwind and crosswind);
- wind turbine operating characteristics;
- the number of turbines and size of the wind farm;
- turbulence intensity;
- frequency distribution of the wind direction (the wind rose).

The extraction of energy from the wind results in an energy and velocity deficit, compared with the prevailing wind, in the wake of a wind turbine. The energy loss in the turbine wake will be replenished over a certain distance by exchange of kinetic energy with the surrounding wind field. The extent of the wake in terms of its length as well as its width depends primarily on the rotor size and power production.

Array losses can be reduced by optimizing the geometry of the wind farm. Different distributions of turbine sizes, the overall shape and size of the wind farm turbine distribution, and turbine spacing within the wind farm all affect the degree to which wake effects reduce energy capture.

The momentum and energy exchange between the turbine wake and the prevailing wind is accelerated when there is higher turbulence in the wind field. This reduces the velocity deficits downstream, and so reduces array losses. Typical turbulence intensities are between 10% and 15%, but may be a low as 5% over water or as high as 50% in rough terrain. Turbulence intensity also increases through the wind farm due to the interaction of the wind with the turning rotors.

Finally, array losses are also a function of the annual wind direction frequency distribution. The crosswind and downwind distances between wind turbines will vary depending on the geometry of the wind turbine locations and the direction of the wind. Thus, array losses need to be calculated based on representative annual wind direction data in addition to wind speed and turbulence data.

The geometry of turbine placement and ambient turbulence intensity have been shown to be the most important parameters affecting array losses. Studies have shown that, for turbines that are spaced 8 to 10 rotor diameters, D, apart in the prevailing downwind direction and five rotor diameters apart in the crosswind direction, array losses are typically less than 10% (Lissaman *et al.*, 1982). Figure 9.6 illustrates array losses for a hypothetical 6 x 6 array of turbines with a downwind spacing of ten rotor diameters. The graph presents array losses as a function of crosswind spacing and turbulence intensity. Results are shown for conditions when the wind is only parallel to turbine rows (turbines directly in the wake of other turbines) and when wind is evenly distributed from all directions.

Array losses may also be expressed as array efficiencies where:

$$\text{Array efficiency} = \frac{\text{Annual energy of whole array}}{(\text{Annual energy of one isolated turbine})(\text{total no. of turbines})} \tag{9.4}$$

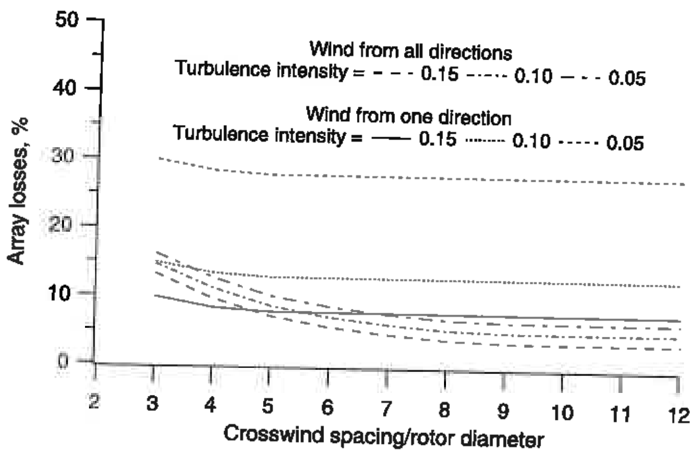

Figure 9.6 Wind farm array losses (after Lissaman *et al.*, 1982). Reproduced by permission of BHR Group Limited

It can be seen that array efficiency is just 100% minus the array losses in percent.

The design of a wind farm requires careful consideration of these effects in order to maximize energy capture. Closer spacing of wind turbines may allow more wind turbines on the site, but will reduce the average energy capture from each turbine in the wind farm.

9.4.2.2 The Calculation of Array Losses – Wake Models

The calculation of array losses requires knowledge of the location and characteristics of the turbines in the wind farm, knowledge of the wind regime, and appropriate models of turbine wakes to determine the effect of upstream turbines on downstream ones. A number of turbine wake models have been proposed. These fall into the following categories:

- surface roughness models;
- semi-empirical models;
- eddy viscosity models;
- full Navier–Stokes solutions.

The surface roughness models are based on data from wind tunnel tests. The first models to attempt to characterize array losses were of this type. A review by Bossanyi *et al.* (1980) describes a number of these models and compares their results. These models assume a logarithmic wind velocity profile upstream of the wind farm. They characterize the effect of the wind farm as a change in surface roughness that results in a modified velocity profile within the wind farm. This modified velocity profile, when used to calculate turbine output, results in appropriately lower power output for the total wind farm. These models are usually based on regular arrays of turbines in flat terrain.

The semi-empirical models provide descriptions of the energy loss in the wake of individual turbines. Examples include models by Lissaman (Lissaman and Bates, 1977), Vermeulen

(Vermeulen, 1980), and Katić (Katić *et al.*, 1986). These models are based on simplified assumptions about turbine wakes (based on observations) and on conservation of momentum. They may include empirical constants derived from either wind tunnel model data or from field tests of wind turbines. They are useful for describing the important aspects of the energy loss in turbine wakes, and, therefore, for modeling wind farm array losses.

Eddy viscosity models are based on solutions to simplified Navier–Stokes equations. The Navier–Stokes equations are the defining equations for the conservation of momentum of a fluid with constant viscosity and density. They are a set of differential equations in three dimensions. The use of the Navier–Stokes equations to describe time-averaged turbulent flow results in terms that characterize the turbulent shear stresses. These stresses can be related to flow conditions using the concept of eddy viscosity. Eddy viscosity models use simplifying assumptions such as axial symmetry and analytical models to determine the appropriate eddy viscosity. These models provide fairly accurate descriptions of the velocity profiles in turbine wakes without a significant computational effort and are also used in array loss calculations. Examples include the model of Ainslie (1985 and 1986) and that of Smith and Taylor (1991).

Figures 9.7 and 9.8 illustrate measured wind speed data behind wind turbines. The graphs also include the results of one of these eddy viscosity wake models. Figure 9.7 shows non-dimensionalized vertical velocity profiles at various distances (measured in rotor diameters) behind a wind turbine. The velocity deficit and its dissipation downwind of the turbine are clearly illustrated. Figure 9.8 illustrates the hub height velocity profiles as a function of distance from the rotor axis for the same conditions. The Gaussian shape of the hub height velocity deficit in the far wake can clearly be seen.

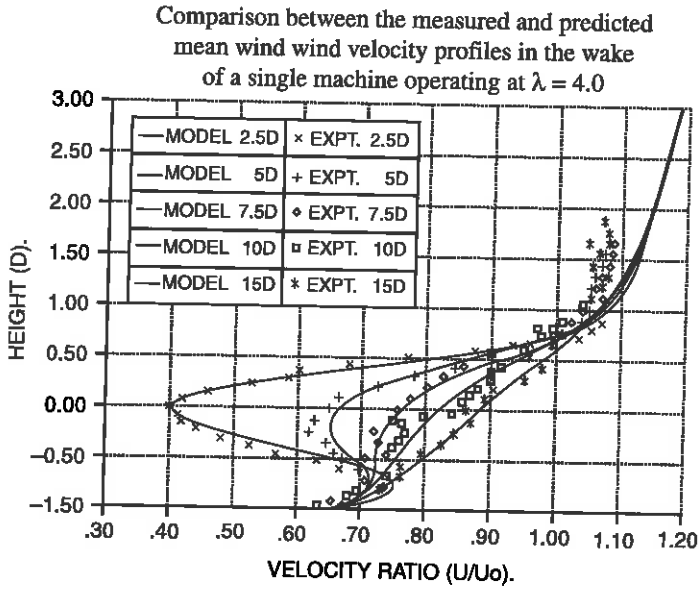

Figure 9.7 Vertical velocity profiles downwind of a wind turbine (Smith and Taylor, 1991); λ, tip speed ratio, U_0, free stream wind speed, D, height with respect to turbine rotor centerline. Reproduced by permission of Professional Engineering Publishing

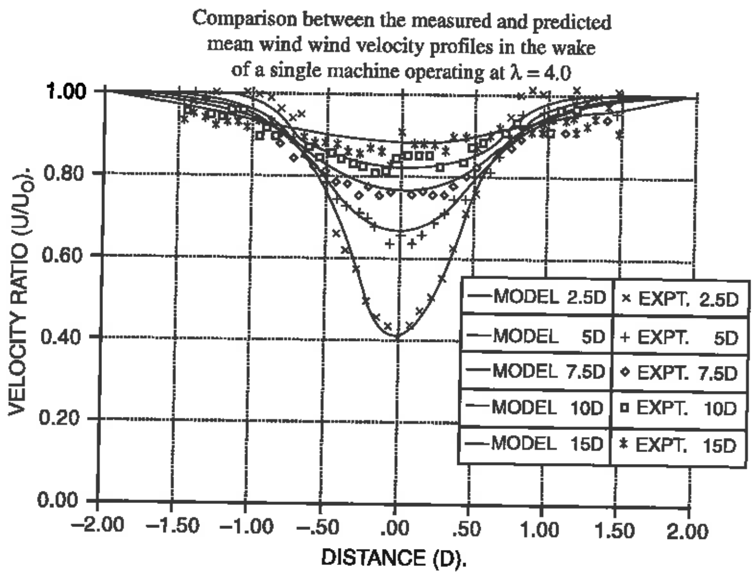

Figure 9.8 Hub height velocity profiles downwind of a wind turbine (Smith and Taylor, 1991); λ, tip speed ratio. Reproduced by permission of Professional Engineering Publishing

Finally, a variety of approaches exist to solving the complete set of Navier–Stokes equations. These models require a significant computational effort and may use additional models to describe the transport and dissipation of turbulent kinetic energy (the k–ε model) to converge to a solution. These models are best suited for research, for detailed descriptions of wake behavior, and to guide the development of simpler models. Examples include models by Crespo *et al.* (Crespo *et al.*, 1985; Crespo and Herandez, 1986; Crespo *et al.*, 1990; Crespo and Herandez, 1993), Voutsinas *et al.* (1993), and Sørensen and Shen (1999).

A number of factors affect the accuracy of the results of applying these models to specific wind farms. When used to calculate wind farm power production, decisions must be made about how to handle the superposition of multiple wakes and the effects of complex terrain on both wake decay and ambient wind speed. A number of the models mentioned above address some of these issues. Typically, multiple wakes are combined based on the combination of the energy in the wakes, although some models assume linear superposition of velocities. The effects of complex terrain may be significant (see Smith and Taylor, 1991) but are more difficult to address and are often ignored.

The use of these models can be illustrated by considering one of the semi-empirical models (Katić *et al.*, 1986) that is often used for micrositing and wind farm output predictions. The model attempts to characterize the energy content in the flow field and ignores the details of the exact nature of the flow field. As seen in Figure 9.9, the flow field is assumed to consist of an expanding wake with a uniform velocity deficit that decreases with distance downstream. The initial free stream velocity is U_0 and the turbine diameter is D. The velocity in the wake at a distance X downstream of the rotor is U_X with a diameter of D_X. The wake decay constant, k, determines the rate at which the wake diameter increases in the downstream direction.

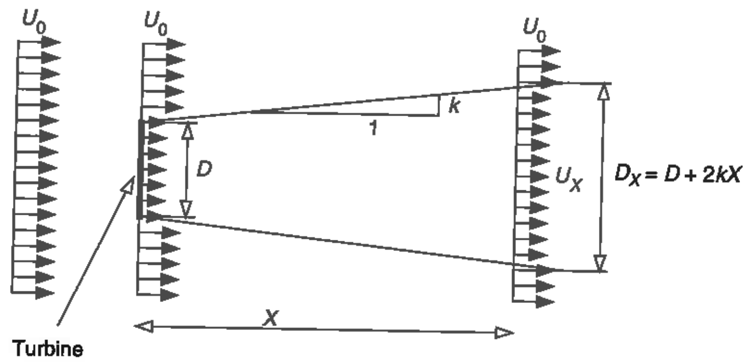

Figure 9.9 Schematic view of wake description (after Katić *et al.*, 1986); U_0, initial free stream velocity; D, turbine diameter; U_X, velocity at a distance X; D_X, wake diameter at a distance X; k, wake decay constant

In this and many other semi-empirical models, the initial non-dimensional velocity deficit (the axial induction factor), a, is assumed to be a function of the turbine thrust coefficient:

$$a = \frac{1}{2}\left(1 - \sqrt{1 - C_T}\right) \tag{9.5}$$

where C_T is the turbine thrust coefficient. Equation (9.5) can be derived from Equations (3.16) and (3.17) for the ideal Betz model. Assuming conservation of momentum, one can derive the following expression for the velocity deficit at a distance X downstream:

$$1 - \frac{U_X}{U_0} = \frac{\left(1 - \sqrt{1 - C_T}\right)}{\left(1 + 2k\frac{X}{D}\right)^2} \tag{9.6}$$

The model assumes that the kinetic energy deficit of interacting wakes is equal to the sum of the energy deficits of the individual wakes (indicated by subscripts 1 and 2). Thus, the velocity deficit at the intersection of two wakes is:

$$\left(1 - \frac{U_X}{U_0}\right)^2 = \left(1 - \frac{U_{X,1}}{U_0}\right)^2 + \left(1 - \frac{U_{X,2}}{U_0}\right)^2 \tag{9.7}$$

The only empirical constant in the model is the wake decay constant, k, which is a function of numerous factors, including the ambient turbulence intensity, turbine-induced turbulence, and atmospheric stability. Katić notes that in a case in which one turbine was upstream of another, $k = 0.075$ adequately modeled the upstream turbine, but $k = 0.11$ was needed for the downstream turbine, which was experiencing more turbulence. He notes also that the results for a complete wind farm with wind coming from multiple directions are relatively insensitive to minor changes in the value of k. A small constant gives a large power reduction in a narrow zone, while a large value gives a smaller reduction in a wider zone. The net effect of varying this parameter, when analyzing wind farm performance at many wind speeds from a variety of directions, is small.